

Field Guide to

# **Optoelectronics and Photonics**

Juan A. Hernández-Cordero  
Mathieu Hautefeuille

SPIE Field Guides  
Volume FG50

J. Scott Tyo, Series Editor

**SPIE PRESS**  
Bellingham, Washington USA

## Library of Congress Cataloging-in-Publication Data

Names: Hernández-Cordero, Juan Arnaldo, author. | Hautefeuille, Mathieu, author.

Title: Field guide to optoelectronics and photonics / Juan A. Hernández-Cordero, Mathieu Hautefeuille.

Description: Bellingham, Washington : SPIE—The International Society for Optical Engineering, [2021] | Includes bibliographical references and index.

Identifiers: LCCN 2021018792 | ISBN 9781510644144 (paperback) | ISBN 9781510644151 (pdf)

Subjects: LCSH: Optoelectronics. | Photonics. | Solids—Effect of radiation on.

Classification: LCC TK8304 .H47 2021 | DDC 621.381/045—dc23

LC record available at <https://lcn.loc.gov/2021018792>

Published by

**SPIE**

P.O. Box 10

Bellingham, Washington 98227-0010 USA

Phone: 360.676.3290

Fax: 360.647.1445

Email: [Books@spie.org](mailto:Books@spie.org)

Web: [www.spie.org](http://www.spie.org)

Copyright © 2021 Society of Photo-Optical Instrumentation Engineers (SPIE)

All rights reserved. No part of this publication may be reproduced or distributed in any form or by any means without written permission of the publisher.

The content of this book reflects the thought of the authors. Every effort has been made to publish reliable and accurate information herein, but the publisher is not responsible for the validity of the information or for any outcomes resulting from reliance thereon.

Cover image credit: GettyImages—Quardia.

Printed in the United States of America.

First printing.

For updates to this book, visit <http://spie.org> and type “FG50” in the search field.

**SPIE.**

## Table of Contents

---

<b>Preface</b>	<b>xi</b>
<b>Glossary of Symbols</b>	<b>xiii</b>
<b>Semiconductor Optics and Optoelectronics I: Fundamentals</b>	<b>1</b>
Maxwell's Equations	1
Electromagnetic Radiation in Vacuum	2
Electromagnetic Radiation in Matter	3
Band Theory: Origin of Energy Bands	4
Band Theory: Classification of Materials	5
Crystallographic Considerations	6
Dispersion Relations	7
Definition of the Photon	8
Common Examples of Semiconductors in Optoelectronics	9
Temperature Dependency	10
<b>Semiconductor Optics and Optoelectronics II: Charge Carrier Statistics</b>	<b>11</b>
Electron Configuration	11
Hund's Rule and Pauli's Exclusion Principle	12
Klechkowsky's Rule (Madelung's Rule)	13
Semiconductor Charge Carriers: Energy Bands	14
Fermi Level	15
Fermi–Dirac Distribution Function	16
Fermi Level and Band Theory	17
Density of States	18
Occupation Probabilities	19
n-Doped and p-Doped Semiconductors	20
Example of Doping: Silicon	21
<b>Semiconductor Optics and Optoelectronics III: Transport Properties</b>	<b>22</b>
Mobility	22
Conduction	23
Diffusion	24
Total Current	25

## Table of Contents

Generation and Recombination: Radiative and Nonradiative	26
Continuity Equations for Carriers	27
<b>p–n Junction</b>	<b>28</b>
Homogeneous Semiconductor	28
Nonhomogeneous Semiconductor	29
Thermodynamic Equilibrium in p–n Junctions: Bands and Carriers	30
Depletion Region	31
Diffusion Voltage and Potential Barrier	32
p–n Junction Bias: Diode	33
Forward and Reverse Bias	34
I–V Characteristics	35
Heterojunctions	36
 <b>Macroscopic Light–Matter Interaction</b>	 <b>37</b>
Boundary Conditions	37
Reflection and Refraction	38
Noether’s Theorem	39
Conservation Laws	40
Light Polarization	41
Fresnel Formulae: Interfaces	42
Extinction and Absorption of Light	43
Transmission	44
Birefringence	45
Dichroism	46
Filters	47
Thin Film Filters	48
Fabry–Pérot Modes	49
 <b>Microscopic and Quantum Light–Matter Interaction</b>	 <b>50</b>
Absorption	50
Scattering	51
Scales in MIE and Rayleigh Scattering	52
Spontaneous Emission	53
Stimulated Emission	54
Plasmons	55

## Table of Contents

---

Quantum Dots	56
<b>Optical Waveguides</b>	<b>57</b>
Light-Guiding Mechanisms	57
Planar Waveguides	58
Waveguide Coupling	59
Diffractive Elements in Waveguides	60
Optical Fibers	61
Light Propagation in Optical Fibers: Multimode, Few-Mode, and Single-Mode	62
Microstructured Optical Fibers: Hollow-Core and Photonic Bandgap Fibers	63
Fiber Bundles	64
Diffractive Elements in Optical Fibers	65
 <b>Optoelectronic Devices</b>	 <b>66</b>
Light-Emitting Diodes (LEDs)	66
LED Efficiency	67
Semiconductor Laser Diodes	68
Diode-Pumped Solid-State Lasers (DPSSLs)	69
Fiber Lasers	70
Photodiodes	71
Avalanche Photodiodes	72
Photomultiplier Tubes	73
 <b>Photonics and Its Applications: Devices</b>	 <b>74</b>
Solar Cells	74
Practical Use of Solar Cells	75
Organic Photovoltaic Devices and Organic LEDs	76
Optical Modulators: Acousto-optic and Electro-optic	77
Spatial Light Modulators (SLMs)	78
Optical Fiber Devices	79
Optical Fiber Sensors	80
Photonic Lanterns	81
 <b>Photonics: Applications of Its Physical Properties</b>	 <b>82</b>
Photonic Crystals	82
Parametric Conversion	83

## Table of Contents

---

UV–VIS Spectroscopy	84
FTIR Spectroscopy	85
Raman Spectroscopy	86
Surface Plasmon Resonance Sensors	87
Optical Time-Domain Reflectometry (OTDR)	88
Distributed Optical Fiber Sensors	89
Laser Micromachining I: Ablation	90
Laser Micromachining II: Photopolymerization	91
Laser Micromachining III: Two-Photon Polymerization	92
<b>Equation Summary</b>	<b>93</b>
<b>Bibliography of Further Reading</b>	<b>99</b>
<b>Index</b>	<b>101</b>

## Preface

---

The material in this *Field Guide to Optoelectronics and Photonics* derives from the notes gathered and created for the lectures taught by the authors at both undergraduate and graduate levels at the School of Sciences and the School of Engineering of the Universidad Nacional Autónoma de México (UNAM). The topics included in the Field Guide are covered in curricular courses such as Biomedical Applications of Optoelectronics (Undergraduate level, School of Engineering), Introduction to Photonics and Radiation–Matter Interaction (School of Sciences, Physics Department), Introduction to Photonics (Graduate level, Graduate Program in Materials Science and Engineering), and in the lectures of Optical Waveguides and Photonic Devices (Graduate level, Graduate Program in Electrical Engineering).

This volume covers the physics of semiconductors, from the materials used in optoelectronics and photonics to charge statistics and transport to p–n junctions and their applications. It then addresses the physics of the interactions between radiation and matter at different levels—macroscopic, microscopic, and quantum—and includes the fundamental concepts of waveguides and fiber optics and photonics devices such as light modulators. It finally highlights important applications of the field in engineering and applied physics.

The text summarizes the scientific and engineering foundations of optoelectronics and photonics and thus can be used as a textbook for college students, although it could be useful for practicing scientists and engineers as well. As with any other text aimed at covering a broad range of topics, some practical details had to be left out due to space constraints. Issues regarding operation of photonic and optoelectronic devices, such as power supply and control, are not covered in the text. The readers are thus left with the task of investigating these aspects that are relevant for practical purposes but in some cases can be very specific to a particular application.

## Preface

---

Juan Hernández-Cordero would like to thank Amado Velázquez-Benítez for his support in teaching the photonics courses, particularly those covering topics on waveguides and devices. Mathieu Hautefeuille would like to give a special acknowledgement to Edwige Bano for her initial introduction to the field of physics of semiconductors (and her precious material) in Grenoble and to Reinher Pimentel for his support as a Teaching Assistant dating back to the initial stages of the courses.

Finally, we both appreciate our interaction with all of the motivated students who have attended our lectures, especially those who stayed longer to experiment with us in our labs. They greatly motivated us to assemble this Field Guide, which we hope will become a useful and handy compendium of some of the most relevant topics related to the myriad of applications of optoelectronics and photonics.

JHC lovingly dedicates this book to Margo and daughters, Lía, Siena, and Katya, who have always been and will remain his source of inspiration. The book is also dedicated to the memory of his mother.

MH dedicates this book to Jimena and sons, Noah and Teo, who patiently support him and whose curiosity always stimulates his will to learn.

**Juan A. Hernández-Cordero**  
Institute of Materials Research, UNAM

**Mathieu Hautefeuille**  
School of Science, UNAM

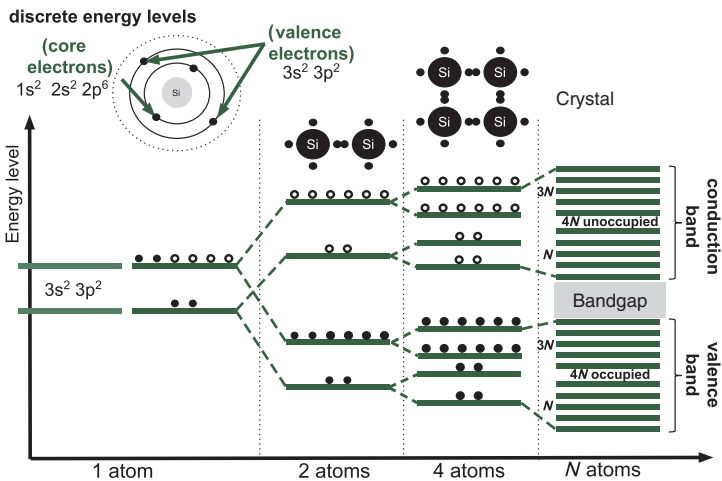


## Band Theory: Origin of Energy Bands

Energy bands exist in solids because of **Pauli's exclusion principle**: in an isolated atom, electrons occupy discrete energy levels. When atoms get closer to each other to form a crystal or a solid, their electrons cannot occupy the same levels of energy, as shown in the diagram.

In a **covalent union** between two atoms, Pauli's exclusion principle would be violated if two electrons were occupying the same energy levels of both atoms when isolated. All electrons thus occupy two discrete, separate levels, starting from lower energies.

When the number of atoms increases, the two levels are subdivided into other **discrete energy levels** very close to each other, forming occupied and unoccupied energy bands, as well as forbidden bandgaps. The bandgaps depend on the lattice constant; a lower-energy band is called a **valence band** (VB), and a greater-energy band is called a **conduction band** (CB).

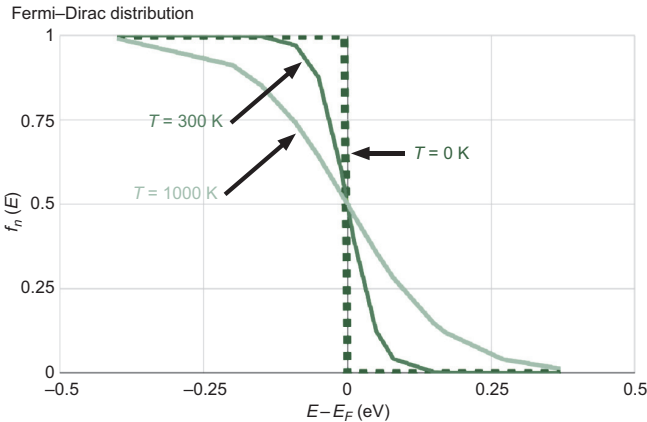


## Fermi–Dirac Distribution Function

In a solid, electrons and holes—like any indiscernible particle with a half-integer spin (called  $\frac{1}{2}$  spin fermions)—obey **Fermi–Dirac statistics**. In a system where a large number of charge carriers fill discrete energy levels complying with Pauli’s exclusion principle, Fermi–Dirac statistics are used to describe the distribution of these particles over the energy states. The distribution is given by

$$f_n(E) = \frac{1}{1 + \exp\left[\frac{E - E_F}{k_B T}\right]}$$

As shown in the plot,  $f_n(E)$  has a strong dependence on temperature  $T$ , and an increase in this parameter, related to higher kinetic energy in the system, will enable a larger number of electrons to reach levels above the Fermi level  $E_F$ .



## Continuity Equations for Carriers

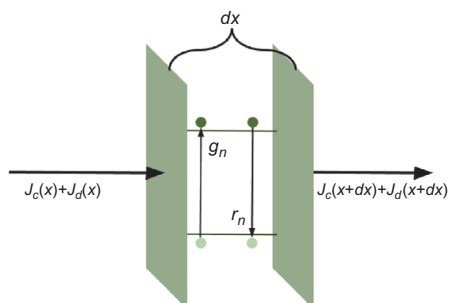
Once the charge carrier distributions and all relevant transport processes (conduction, diffusion, generation, and recombination) have been defined, it is possible to write **continuity equations** for both types of carriers. These equations govern the general conditions of **dynamic equilibrium** and are written as

$$\frac{\partial n}{\partial t} = n\mu_n \frac{\partial E}{\partial x} + \mu_n E \frac{\partial n}{\partial x} + D_n \frac{\partial^2 n}{\partial x^2} + g_n - r_n$$

$$\frac{\partial p}{\partial t} = \underbrace{-p\mu_p \frac{\partial E}{\partial x} - \mu_p E \frac{\partial p}{\partial x}}_{\text{Drift}} + \underbrace{D_p \frac{\partial^2 p}{\partial x^2}}_{\text{Diffusion}} + g_p - r_p$$

These equations describe all phenomena perturbing the unbound carriers of a semiconductor material. The first two terms define the drift process of the carriers under the influence of an electric field  $\mathbf{E}$  for electrons  $n$  and holes  $p$ . The remaining terms describe the diffusion process and account for the generation ( $g_n, g_p$ ) and the recombination ( $r_n, r_p$ ) rates.

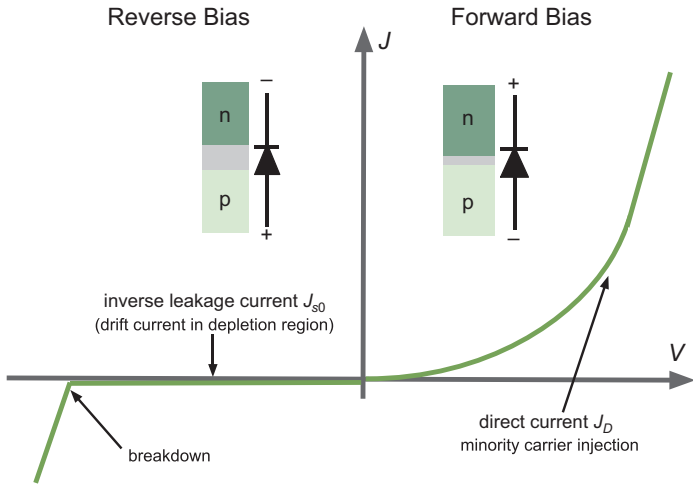
Physically, as illustrated below, these differential equations essentially depict the time variation of the carrier densities due to the difference between the incoming and outgoing flux of free carriers ( $J = J_c + J_d$ , where  $J_c = J_{cond}$ , and  $J_d = J_{diff}$ ) in the material, considering also a possible generation and recombination.



## I-V Characteristics

The **total current density**  $J_D$  is expressed as a function of the bias forward voltage  $V$  by the following equation:

$$J_D = J_{s0} \left[ \exp\left(\frac{eV}{kT}\right) - 1 \right]$$



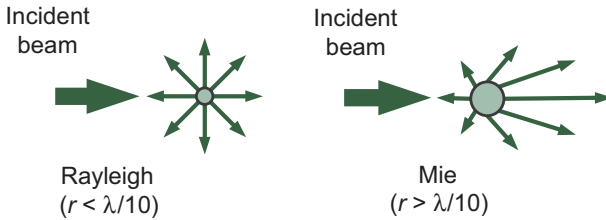
When defining the **saturation current**  $J_{s0}$  in detail, it becomes clear that this current depends on the semiconductor material used to build the diode and is usually expressed as a function of the bandgap-dependent potential  $V_g = \frac{E_g}{e}$ . This leads to

$$J = J_0 \exp\left[\frac{e(V - V_g)}{kT}\right]$$

## Scales in MIE and Rayleigh Scattering

---

The effects of **elastic scattering** depend on the **size of the scatterer** (e.g., a **particle**) relative to the **wavelength** of light. For a particle radius much smaller than the wavelength ( $r < \lambda/10$ ), scattering is known as **Rayleigh scattering**. At larger scales, the scattering is described by **Mie scattering** theory ( $r > \lambda/10$ ). As shown in the figure, light can be scattered in all directions.

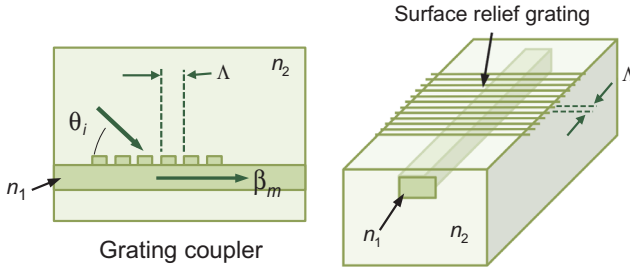


Rayleigh scattering arises due to small particles such as atoms or molecules, and photons are scattered in all directions **uniformly**. This effect varies inversely with wavelength ( $\sim \lambda^{-4}$ ) and is therefore more noticeable at shorter wavelengths. A typical example of Rayleigh scattering is observed in the atmosphere: sunlight is scattered by **atmospheric particles**, resulting in the seemingly blue tones in the sky.

Interaction of light with larger particles leads to Mie scattering effects, which are not strongly wavelength dependent. Photons are not scattered uniformly, showing a dependence on the **angle of incidence** of light. This angle dependency becomes stronger as the size of the particle increases. Examples of Mie scattering effects can be observed from light scattered by clouds or fog, which results in a seemingly white tone.

## Diffractive Elements in Waveguides

Diffraction gratings in planar waveguides are used as **light-coupling devices**. Such a grating is realized by introducing **periodic corrugations** on the surface of the waveguide (surface relief gratings), or by **periodically modulating** its **refractive index**. Because the grating modulates the phase of the incoming wave, light can be coupled into (or out of) the waveguide. Light coupling among propagating modes is also possible.



As illustrated in the figure, **grating couplers** allow for matching the phase of an incident beam (incident angle  $\theta_i$ ) with the propagation constant of a guided mode ( $\beta_m$ ). The **phase-matching condition** is given by

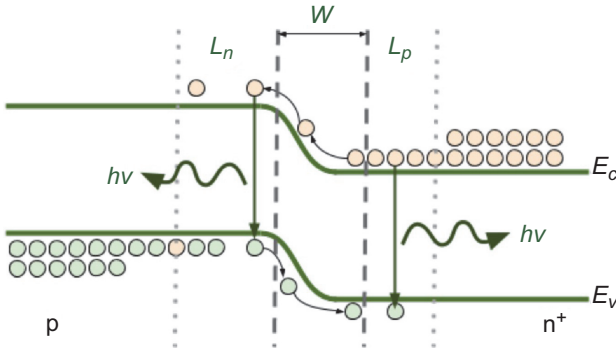
$$\beta_m = n_2 k_0 \cos(\theta_i) + \frac{2\pi q}{\Lambda}$$

where  $k_0$  is the wavenumber,  $q$  is the **diffraction order** (an integer), and  $\Lambda$  is the grating period.

Light propagating within the waveguide can be coupled to a **backward-propagating mode** upon interaction with a grating. This interacting structure is known as a **Bragg grating** and reflects light at wavelengths satisfying the condition  $\lambda_B = 2\Lambda/q$ . Bragg reflectors are commonly used to provide feedback in **semiconductor laser diodes**, yielding DBR (distributed Bragg reflector) or DFB (distributed feedback) laser devices. Such structures can deliver **single-mode laser operation**.

## Light-Emitting Diodes (LEDs)

The basic structure of a **light-emitting diode** (LED) is a **p–n junction** of a direct-bandgap semiconductor in a **forward-bias** configuration. As shown in the band energy diagram, the injection of minority carriers creates three emitting regions:  $W$ ,  $L_n$ , and  $L_p$ . Since the **injection rate** of the  $n^+$  region is greater than that of the p region, the p-doped region presents a greater **recombination rate** and thus a higher emission. This is usually the emitting side of a LED.



The LED optical output power  $P_{out}$  is given as a function of the **photon energy**  $h\nu$ , the **external quantum efficiency**  $\eta_{ext}$ , its cross-sectional area  $A$ , the radiative lifetime  $\tau_r$ , and the excess minority carrier  $n - n_0$ :

$$P_{out} = \eta_{ext} h\nu A \int \frac{n - n_0}{\tau_r} dx$$

In general, LEDs show low external efficiencies due to total internal reflection: the high **refractive-index mismatch** between semiconductors ( $\sim 3.5$ ) and air causes a low-TIR angle. This must be corrected with different approaches such as **index gradients**, rough surfaces instead of flat surfaces, or even dome-shaped packaging.

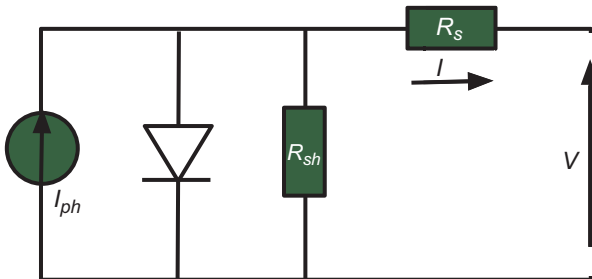
## Solar Cells

Solar cells are **semiconductor devices** that convert the energy of light into electricity, using the **photovoltaic effect** (PV). A PV cell or solar cell is based on a photodiode with or without external bias, and the **total electrical current**  $I$  [ $\text{A}/\text{cm}^2$ ] generated by the PV cell is given by

$$I = I_{ph} - I_s \left[ \exp \frac{q(V + R_s I)}{\eta k T} - 1 - \frac{V + R_s I}{R_{sh}} \right]$$

where  $I_{ph}$  is the photogenerated current due to light absorption,  $I_s$  is the reverse saturation current,  $\eta$  is the ideality factor (caused by undesired **recombinations** inside the device),  $k$  is Boltzmann's constant,  $q$  is the charge of the electron,  $R_s$  is the parasitic series,  $R_{sh}$  is the shunt resistance, and  $T$  is the temperature of the cell. The representation of a typical I-V curve of a solar cell is shown on the following page.

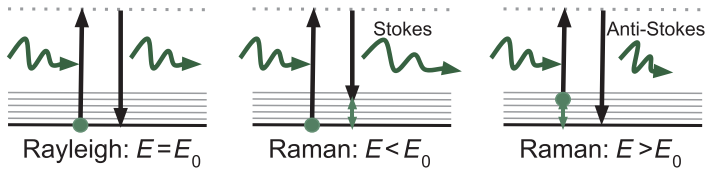
A **solar cell** can be represented by an electrically equivalent circuit model using simple discrete elements, as depicted in the diagram below. A solar cell biased by a voltage  $V$  is thus represented by a current source  $I_{ph}$  in parallel with a diode and a shunt resistance  $R_{sh}$  that, together with a series resistance  $R_s$ , account for the fact that the solar cell is not ideal.





## Raman Spectroscopy

Raman spectroscopy is another analytical tool to analyze materials using light in a non-invasive fashion. It is based on **Raman scattering**, in which a very small amount of light is scattered by matter following an inelastic process. (Raman scattering is represented in only about 1 out of  $10^7$  scattered photons coming from elastic Rayleigh-scattered light!)



As Raman scattering is caused by a **nonresonant inelastic process**, the energy of Raman-scattered light differs from that of the incident light  $E_0$ . The energy can be either lower (Stokes Raman scattering) or greater (anti-Stokes Raman scattering) than that of  $E_0$ . Practically speaking, because the intensity of Raman scattering is very weak, Rayleigh-scattered light must be filtered using Raman spectroscopy, and only Stokes Raman-scattered photons are registered (i.e., they have greater wavelengths than the excitation wavelength).

For simplicity, only the energy/wavelength difference is considered for the **Raman spectrum**. This difference is therefore represented as the intensity of the scattered light versus the wavenumber (called the **Raman shift**). For example, the Raman peak at 547.14 nm of ethanol is obtained by a 532-nm excitation wavelength and is represented by the wavenumber  $520 \text{ cm}^{-1}$ .

**Raman spectroscopy** relies on a material's ability to scatter light in an **inelastic** manner. The position of a Raman-scattered intensity peak identifies a particular molecular structure. The scattering intensity is related to the substance concentration, the width of the intensity peak indicates the **crystallinity** of the material, and a shift in this peak is a sign of stress.

## Equation Summary

---

### Maxwell's equations:

For a medium with free charge density  $\rho_V$ :

Maxwell–Gauss:  $\nabla \cdot \mathbf{D} = \rho_V$ , or  $\text{div } \mathbf{D} = \rho_V$

Maxwell's magnetic flux:  $\nabla \cdot \mathbf{B} = 0$ , or  $\text{div } \mathbf{B} = 0$

Maxwell–Ampère:

$$\nabla \times \mathbf{H} = \mathbf{J}_f + \frac{\partial \mathbf{D}}{\partial t}, \text{ or } \text{rot } \mathbf{H} = \mathbf{J}_f + \frac{\partial \mathbf{D}}{\partial t}$$

Maxwell–Faraday:  $\nabla \times \mathbf{E} = -\frac{\partial \mathbf{B}}{\partial t}$ , or  $\text{rot } \mathbf{E} = -\frac{\partial \mathbf{B}}{\partial t}$

Electric flux density:  $\mathbf{D} = \epsilon_0 \mathbf{E} + \mathbf{P}$

Magnetic flux density:  $\mathbf{B} = \mu_0(\mathbf{H} + \mathbf{M})$

where the vector fields  $\mathbf{P}$  and  $\mathbf{M}$  are the polarization density and the magnetization density, respectively, of the medium.

### Wave equation (D'Alembert):

$$\nabla^2 \mathbf{E} - \mu_0 \epsilon_0 \frac{\partial^2 \mathbf{E}}{\partial t^2} = 0$$

(The same form is obtained for the magnetic field.)

### Lorentz's force law:

$$\mathbf{F}_L = q(\mathbf{E} + \mathbf{v} \times \mathbf{B})$$

### Varshni relation:

$$E_g(T) = E_g(0 \text{ K}) - \frac{\alpha T^2}{T + \beta} \quad (\alpha \text{ and } \beta \text{ are constants})$$

### Fermi–Dirac distribution:

$$f_n(E) = \frac{1}{1 + \exp \left[ \frac{E - E_F}{k_B T} \right]}$$

## Equation Summary

---

### Fiber gratings:

Bragg gratings (peak reflectivity):

$$\lambda_B = 2n_{eff}\Lambda$$

Long-period gratings (phase-matching condition):

$$\lambda_i = (n_{01} - n_{cl}^{(i)})\Lambda$$

### Surface plasmon resonance (SPR) sensors:

$$\text{SPR angle : } \varphi_{\text{SPR}} = \sin^{-1} \left( \frac{1}{n_p} \sqrt{\frac{n_e^2 n_g^2}{n_e^2 + n_g^2}} \right)$$

### Laser micromachining:

$$\text{Laser ablation threshold: } I_{th} = I_0 \exp \left( \frac{-2G_w^2}{d_b^2} \right)$$



**Juan A. Hernández-Cordero** received his B.Sc. degree in electrical engineering from the Universidad Nacional Autónoma de México (UNAM). He earned Master's and Ph.D. degrees from the Division of Engineering at Brown University and spent a year as a Postdoctoral Research Associate at the Laboratory for Lightwave Technology at Boston University. He is currently a fulltime tenured researcher at the Materials Research Institute (IIM) of the UNAM, where he has established the Laboratory for Photonic Devices and Optical Fiber Sensors. Since 2001, he has lectured in Optoelectronics, Photonics, and Optical Waveguides in undergraduate and graduate programs in physics and electrical engineering at the UNAM. His fields of interest include optical fiber sensors, fiber lasers, and photonic devices for biomedical applications.



**Mathieu Hautefeuille** is a Professor in the Physics Department of the School of Science at Universidad Nacional Autónoma de México (UNAM), México. He received his B.Eng.Sc. and M.Eng.Sc. in Electronic Engineering from the Institut Polytechnique de Grenoble, France and his Ph.D. in Microelectronics Engineering from University College Cork, Ireland. He lectured on Optoelectronics and Electronic Instrumentation & Measurements, as well as the Physics of Semiconductors and Interaction of Radiation–Matter between 2011 and 2020 and has focused on applying these topics in his research on laser microfabrication of biomaterials, biosensors development, and imaging. He was responsible for the LaNSBioDyT National Lab at UNAM between 2015 and 2020 and has contributed more than 40 articles to international journals.